Soft Matter

SYNOPSIS

Nicolae Hurduc*, Bogdan C. Donose*, Alina Macovei, Cristina M. Paius, Constanta Ibanescu, Dan Scutaru, Mathieu Hamel, Norica Branza-Nichita*, Licinio Rocha*

Direct observation of athermal photofluidisation in azo-polymer films
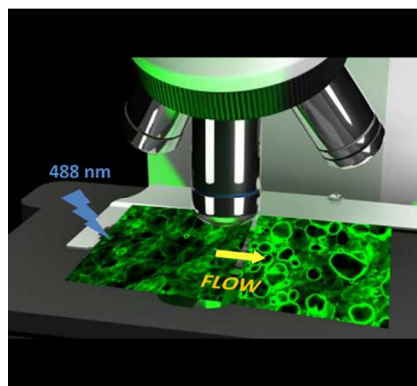
Light induced fluidization of azopolysiloxane: exposure to 488 nm light generates instantaneous mass transfer as result of *trans-cis* isomerization in unsubstituted azophenol polymers. p-Nitro azophenol in the side chain is responsible for the suppression of athermal photofluidization. Viscoelastic mapping confirms the changes of rheological properties upon exposure to 365 nm light.

Journal Name

ARTICLE

DIRECT OBSERVATION OF ATHERMAL PHOTOFLUIDISATION IN AZO-POLYMER FILMS

Nicolae Hurduc[a]*, Bogdan C. Donose[b]*, Alina Macovei[c], Cristina Paius[a], Constanta Ibanescu[a], Dan Scutaru[a], Mathieu Hamel[d], Norica Branza-Nichita[b]*, Licinio Rocha[d]*

The surface relief gratings (SRGs) can be generated when azo-polymer films are exposed to laser beams interference as a result of mass migration. Despite considerable research effort over the past two decades this complex phenomenon remains incompletely understood. Here we show, in premiere, the athermal photofluidisation of azo-polysiloxane films exposed to 488 nm light, directly monitored by optical microscopy. A process of surface relief erasure occurring in parallel with its inscription was also observed during laser irradiation. We therefore propose a new mechanism of SRG formation, based on three different processes: (1) the polymer photo-fluidization in the illuminated regions (2) the mass displacement from illuminated to dark regions and (3) the inverse mass displacement, from dark to illuminated regions. The mechanical properties of the films during UV light irradiation were investigated by classical rheology and, in premiere, by using amplitude modulation-frequency modulation atomic force microscopy (AM-FM AFM).

(**The article is dedicated to Almeria Natansohn**)

Introduction

Almost 20 years ago, Natansohn et al.[1] and Kumar et al.[2] reported independently one of the most exciting behaviours of azo-polymers: the capacity to generate surfaces with sinusoidal topography as a consequence of light irradiation through an interference pattern. Surface relief gratings (SRG) are the result of the *trans-cis* isomerisation of the azobenzene groups, either linked to a polymeric chain[1-7] or as part of azo dye doped polymers (guest-host systems).[8] Despite the large number of studies attempting to characterize this process, the mechanism underlying the SRG formation is still unclear. In our opinion, elucidation of the mechanisms of the azobenzene photophysics has been hindered by the controversy over the athermal photofluidization process. This phenomenon has been a subject of many debates, recent experimental and theoretical studies showing contradictory results which question the validity of the concept.[9-13]

Several models have been proposed so far, such as: the isomerisation pressure[14], the gradient electric force[15], the permittivity gradient[16], the asymmetric diffusion (migration)[17,18], the mean-field model,[19] the theory of light-induced deformation[20], the cage-breaking model[21], or the statistical model based on fundamental molecular dipole[22] - none of them succeeding to comprehensively explain the surface relief formation. In the case of continuous laser irradiation, it is clear that the nanostructuration mechanism involves the directional displacement of the material from the exposed to the masked regions.[17, 23] Nevertheless, due to the very low flow rates of the material during laser irradiation, the mass displacement could not be directly observed so far. For example, in the case of SRG formation, polymer migration rates lower than 1 nm/s were reported.[5,24] Another difficulty concerning the direct observation of the photo-fluidization process is the light wavelength domain in which it is expected to take place (365-488 nm).

The interest to elucidate the azo-polymers nano-structuration is justified by their very recent applications in a variety of areas, such as biology, solar energy conversion and plasmonics. In biology, the nanostructured azo-polymeric films can be used as support for cell cultures, acting as a 3D extracellular matrix

(ECM).[25-27] Understanding the ability of cells to process and respond to different signals received from the ECM was the objective of many research studies reported lately.[28-32] The ECM geometry and rigidity can influence cell adhesion, with direct consequences on cell morphology and migration capacity, tissue architecture and regeneration.[28, 33] Moreover, it has been reported that stem cells fate/differentiation can be induced by the flexibility and geometry of ECM.[34] The major advantages provided by the use of azo-polymers as ECM are the simplicity of the one-step SRG formation, in contrast with classical nanolithography requiring many preparation steps[35-38] and the relief geometric parameters, which are impossible to achieve by other methods. In the field of solar energy conversion the nanostructured azo-polymeric films can be used as templates for metallic colloids employing layer-by-layer deposition.[39, 40] Plasmonics is a relatively new research field that uses the optical properties of metallic nanostructures to manipulate the light at nanometric scale. Photo-sensitive materials, such as azobenzene, can interact with the light field localized at the metal interface, providing important information about the spatial light distribution.[41-44]

In this paper, we report the direct optical microscopy observation of athermal photofluidisation taking place in azo-polysiloxane films. We also evidenced another interesting process consisting in the surface relief erasure during the SRG inscription, which results in reduction of the profile amplitude. Based on these observations we propose a new mechanism of SRG formation relying on three simultaneous processes: (1) the polymer photo-fluidization in illuminated regions, (2) the mass displacement from illuminated to dark regions and (3) the inverse mass displacement from dark to illuminated regions. The mechanical properties of the films during UV light irradiation were investigated by classical rheology and, in premiere, in real-time by viscoelastic mapping AM-FM AFM. The results evidenced important differences in the magnitude of elastic moduli as a consequence with the light interaction. The modification of the Young's modulus value using the light has a very interesting potential application in the cell cultures field. Using different wave lengths the flexibility of the azo-polysiloxane cell substrate can be modified in a controlled manner, thus allowing the real time investigation of the cell response right through changes in the mechanical properties of the extracellular matrix.

Results and discussion

Two types of azo-polymers were investigated in this study, having a flexible (polysiloxane) or rigid [poly(chloromethyl styrene)] main chain. Both polymers contain chlorobenzyl groups in the side chain, modified by a substitution reaction with different azo-phenols. Three types of azo-compounds were connected to the polysiloxanic chain: 4-phenylazophenol [**Azo-Psi**], 4-((4'-nitrophenyl)azo)phenol [**NO₂ -Azo-Psi**] and 4-((4'-hydroxiphenyl)azo)benzonitrile [**CN-Azo-Psi**]. The chemical structure and synthesis route of these azo-polysiloxanes are shown in Scheme 1. Details of polymer synthesis and characterization were reported previously.[45] The poly (chloromethyl styrene) [**PCMS**] modification with the 4-phenylazophenol [**Azo-PCMS**] has been done in similar conditions as in the case of the polysiloxane.

The main characteristics of the studied polymers are summarised in Table 1. The UV-VIS absorption spectra, corresponding to the synthesized azo-polysiloxanes are presented in Figure S1 (Supplementary Information).

The azo-polymers can be used as support for cell cultures, a property investigated by our laboratory using plane and nano-structured surfaces.[27] These studies have shown that the chemical structure of the azo-polymer has an important impact on cell adhesion and proliferation, independent of the surface geometry.
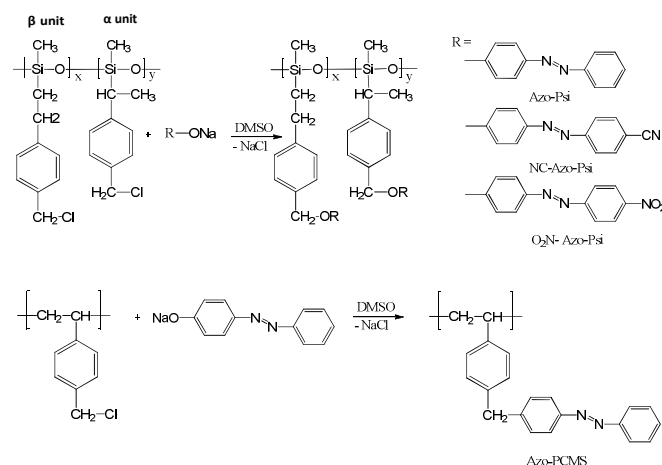
Scheme 1. Synthesis route of the azo-polysiloxanes and azo-PCMS. The starting polysiloxane contains two types of structural units, named α and β, with the x/y ratio = 3/1.

Table 1. The main characteristics of the synthesized polymers.

Spl. code	Azo-group substituent	Substitution degree (%)	Mn	Tg [a] [°C]
1	4-phenylazophenol **(Azo-Psi)**	85	10,300	32
2	4-((4'-nitrophenyl) azo)phenol **(NO₂-Azo-Psi)**	82	11,250	48
3	4-((4'-hydroxiphenyl) azo)benzonitrile **(CN-Azo-Psi)**	80	11,200	65
4	4-phenylazophenol **(Azo-PCMS)**	98	11,800	87

[a] DSC method

During the evaluation of the interactions between the azo-polysiloxanic film and the cells, a very interesting phenomenon was observed in the case of Sample 2 (Table 1), when 488 nm light (filtered HBO lamp source) was used to visualize the actin filaments. After a few seconds of microscopic visualization at room temperature, the azo-polysiloxane film began to flow (Video 1 – Supplementary Information). In our opinion the polymer «melting»

is the result of the athermal photo-fluidization induced by isomerisation of the *trans-cis-trans azo-groups*. To our knowledge, this is the first report showing that a fluid state induced by light can be directly observed by optical microscopy (Figure 1 and Video 1). This behaviour was anticipated by our group since 2007, when only the consequences of photofluidization were evidenced by AFM[46] and a new concept of *conformational instability* was introduced to explain the difficulty/impossibility to generate a solid phase. However, we have not succeeded to demonstrate it conclusively so far. The observation described above strongly suggests that this conformational instability is the result of the continuous *trans-cis-trans* isomerization cycles of the azobenzene groups following their interaction with the UV/VIS light. Since the fluorescence dye was "fixed" to the polymer film using a standard PFA fixation procedure, the possibility that the dye would migrate upon light excitation is excluded.

Video 1. Athermal photo-fluidization of the azo-polysiloxanic film corresponding to NO2-Azo-Psi. The video shows the polymer film fluidization as a result of its interaction with the 488 nm light (microscope HBO lamp source). The displacement of cells during the film fluidization can be observed. – Supplementary Information
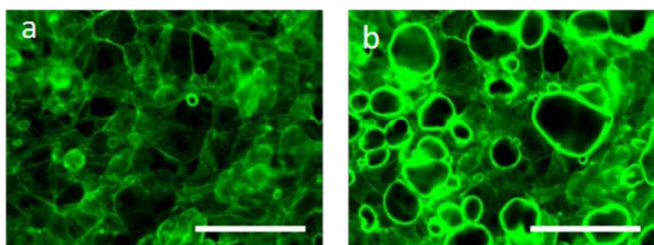

Fig. 1. Athermal photofluidisation of the azo-polysiloxanic film (NO2-Azo-PSi) during exposure to 488 nm light. Actin filaments in HepaRG cells seeded on the polymer film were stained with Alexa Fluor 488-labeled Phalloidin and visualized for 2 (a) or 8 (b) seconds. Scale bar is 100 μm

To verify if the intriguing behaviour of the NO_2-Azo-PSi film when exposed to 488 nm light is an intrinsic property of the polymer or is induced by the growth of the cell monolayer, the experiment was repeated using a similar plane film in the absence of cells. To enable monitoring the process at the same wavelength, the polymer was stained by incubation with Alexa Fluor 488-labeled goat antibody. As shown in Video 2 (Supplementary Information) the athermal photofluidisation was clearly detected again demonstrating that it occurs independently of the film interaction with cells.

Video 2. Athermal photofluidization of a 1 μm thick NO_2-Azo-Psi film stained with Alexa Fluor 488-labeled goat antibody.

Interestingly, none of the other two types of azo-polysiloxanes responded to 488 nm light. This observation suggests that the *cis-trans* equilibrium value, characteristic to each azo-group, plays an important role in fluidization process.

To gain more insights into the athermal photofluidization, a series of complementary studies were performed using rheological methods, AFM, UV-VIS spectroscopy and laser irradiation.

The analysis of the rheological properties of the polymers in the presence and absence of light is expected to provide very important mechanistic information concerning the photo-fluidization process. Based on the results obtained by optical microscopy, the rheological studies in the presence of light should ideally employ irradiation of samples at the same wavelengths.

As the rheometer is not equipped with light sources in the visible range, the studies were conducted using the closest wavelength of 365 nm. In addition, it should be noted that the minimum thickness of the film used in rheological tests was around 400 μm. The complex modulus (G*) values corresponding to samples Azo-Psi and NO_2-Azo-Psi samples are in the range of 8.5 - 10.5 MPa, evidencing a behaviour standing between soft (G* ≤ 1 MPa) and rigid materials (G* ≥ 1 GPa).[36]

When the Azo-Psi sample is UV irradiated at 25 °C (Figure 2a) a slow diminution of the complex modulus (G*) is observed accompanied by an increase of the tan δ value; however, the system is not in a real fluid state yet, since the tan δ value is not above 1. When the temperature is increased to 37 °C an important decrease of the G* value is evidenced during the UV exposure. Accordingly, the tan δ value increases above 1, reflecting the fluid state of the film. This suggests that the UV light induces *trans-cis-trans* isomerisation cycles of the azo-groups, thus increasing the movement of the polymer chain segments.
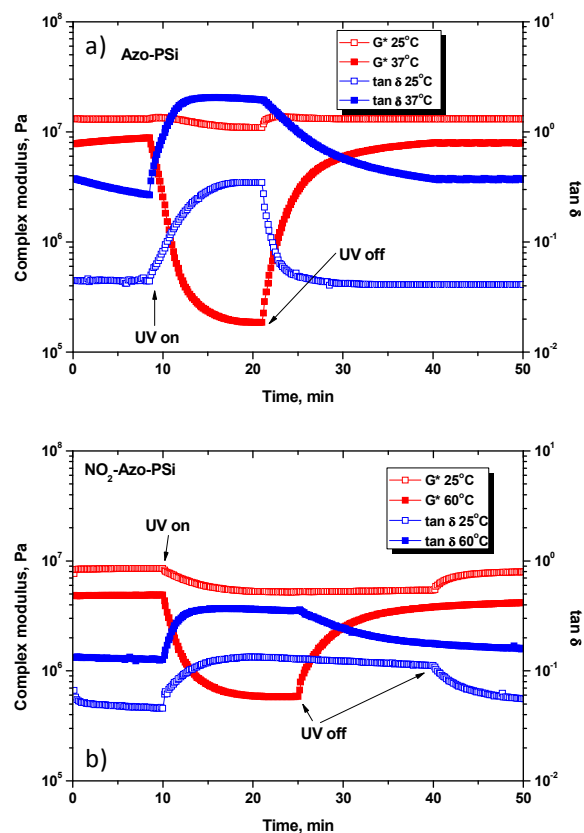

Fig. 2. Rheological behaviour of the Azo-Psi (a) and NO_2-Azo-Psi (b) samples during UV irradiation (365 nm) at different temperatures. Sample film thickness was 400 microns. After 10 minutes from the beginning the

rheological test the UV light source was switched on and the film was irradiated at constant temperature until the stabilization of the complex module value.

This rheological behaviour of the Azo-Psi sample confirms the concept of *conformational instability* which we have proposed previously.[46]

A similar variation of the G* and tan δ values was observed during the UV irradiation of the NO₂-Azo-Psi sample (Tg = 48 °C, Table 1). However, a real fluid state was not obtained in this case, despite sample heating above the Tg value, the tan δ value remaining below 1. This intriguing rheological behaviour can be explained by the differences of the photo-isomerization rates and the trans-cis equilibrium values corresponding to unsubstituted and para NO₂-substituted azo groups.

We next performed viscoelastic mapping AM-FM AFM[47] before, during and after light irradiation. This method not only offers calibrated quantitative evaluation of sample viscoelasticity (as it provides data on loss tangent) but it also allows the possibility to monitor the mechanical properties in real-time and at the same location. Scanning the film surface in the fluid state was practically impossible, due to capillary forces trapping the probe into the polymer mass. Therefore, we applied irradiation conditions that only diminish the modulus value, without a full fluidization of the sample. In order to obtain comparable results with the rheology study, the azo-polysiloxane films were irradiated using an UV lamp (365 nm). A first general observation regarded the mechanical properties measured by AFM, which were different for very thin films (500-2000 nm), compared to the thick films (above 400 µm) tested by rheometry. Rheometry shearing elasticity moduli were in the MPa range while the AM-FM AFM compressive moduli were measured to be the GPa domain.
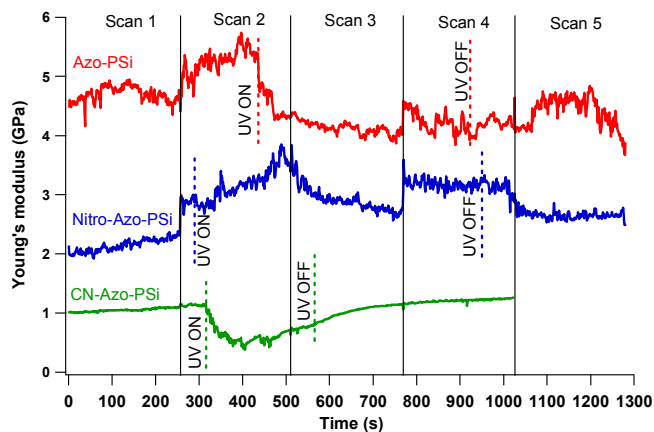

Fig. 3. Young's modulus variation over time during five scans of Azo-Psi, NO₂-Azo-PSi and CN-Azo-Psi thin films at the same location

Figure 3 shows general trends in moduli and topography of the Azo-Psi, NO₂-Azo-Psi and CN-Azo-PSi samples, before, during and after irradiation with 365 nm light. For the first two samples, the first pass (scan 1) of the scanning cantilever induced an increase in the modulus of approximately 1GPa, which is considered to be an effect of sample compression upon

contact with the tip. The compression induced increase of moduli can be observed for both polymers at the beginning of Scan 2. The CN-Azo-PSi polymer seemed to maintain its mechanical properties after the first pass. Azo-PSi reacted immediately to irradiation, the modulus dropping from 5.8 GPa to 4 GPa, while Nitro-Azo-Psi reacted slower, the drop of modulus (approximately 0.8 GPa) starting in Scan 3, 200 seconds after the start of irradiation. Overall, the Azo-PSi and CN-Azo-Psi polymers have similar behaviours, partially recovering after irradiation. In striking contrast, the NO₂-Azo-Psi polymer softens in scan 3 and hardens in the subsequent pass, suggesting plastic deformation. After the UV light is turned off, the polymer softens again. This opposite behaviour of polymers with substituted azobenzene in their structure suggests that the photofluidisation mechanism depends on the nature of the substituents and probably, on the percentage of *cis* and *trans* isomers.

It is worth noting that the topography of the sample changes in terms of RMS roughness upon irradiation and relaxation, dropping from 1.0 to 0.6 nm for Azo-PSi, 11.5 to 9.3 nm for NO₂-Azo-PSi and 3.1 to 1.7 nm for CN-Azo-PSi polymers (Table S2).

The evolution of the mechanical properties under UV irradiation and the relaxation in the dark are critical to understand the photo-fluidisation mechanisms. To our knowledge, the recordings of moduli evolution upon UV excitation, employing AM-FM viscoelastic mapping are a premiere. The AFM micrographs corresponding to the height and Young's modulus of the synthesized polymer films are presented in Figures S2 and S3 respectively.

The modification of the Young's modulus value using light may find potential, interesting bio-applications in cell development research. It is possible to control the softness of the azo-polysiloxane film cell substrate, using different light wavelengths, and further monitor in real time the cell response to changes of the extracellular matrix mechanical properties.

During the azo-polysiloxane SRG inscription another surprising behaviour of azo-polysiloxanes was observed. In the case of the Azo-Psi polymer film a parallel erasure process, leading to the reduction of the relief amplitude, was identified. The surface relief was generated using a 488 nm laser polarized horizontally (180 mW·cm⁻²). As shown in Figure 4, the diffraction intensity decreases after 50-60 min of irradiation, indicating the surface erasure. The experiments were performed using 650 nm thick films and different illumination times in order to correlate the diffraction curves with the evolution of the surface amplitude. The process was further confirmed by AFM, a reduction of the relief amplitude from 239 to 114 nm being observed. These amplitude modulations were detected when maximum and minimum diffraction intensities were reached (239 nm after irradiation for 1 hour and 114 nm after irradiation for 2 hours). In this case, the erasure process stops after 2 hours of irradiation and the imprinting restarts. As a consequence, after 3 hours of irradiation the relief amplitude increases to 180 nm. Figure 4 (a, b) shows typical profiles of the surface modulation measured by AFM.

This unexpected behaviour suggests that a process of inverse mass displacement from dark to illuminated regions takes place. Very recently, Accary and Teboul[48] proposed a similar mechanism, using

molecular modelling simulations. The authors attributed the phenomenon to a local material softening occurring around isomerising azobenzene molecules. The process was shown to increase with the illumination intensity, i.e. with the azobenzene isomerisation rate, favouring local molecular reorganisations against a long range material migration. In our case, the reverse migration occurs after a certain time while the illumination intensity is maintained constant, evidencing a competition between the two processes.
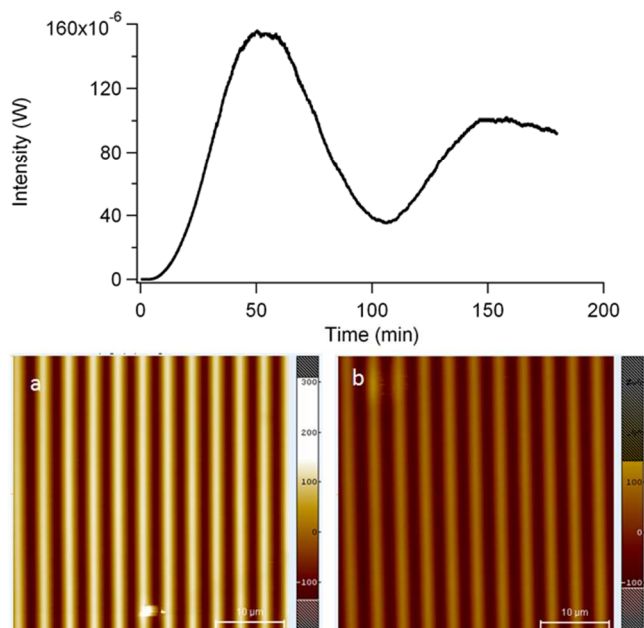

Fig. 4. Diffraction curve reflecting the formation and erasure of the surface relief of a film corresponding to Azo-Psi polymer after 3hours of irradiation. AFM micrograph of the surface relief obtained when illumination is stopped after 1 hour (maximum of diffraction efficiency) (a) or after 2 hours (minimum of diffraction efficiency during erasing) (b).
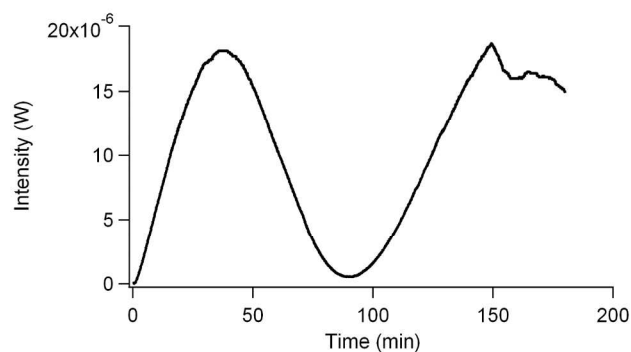

Fig. 5. Diffraction curve reflecting the formation and erasure of the surface relief of a film corresponding to Azo-PCMS polymer after 3 hours of irradiation.

The inscription-erasing cycles were evidenced for all the investigated azo-polysiloxanes as a function of the chemical structure, the irradiation time for a complete cycle being different. As one can see in Figure S4, for NO_2-Azo-Psi sample, only 75 minutes of irradiation are necessary for a complete inscription-erasing cycle. To determine whether the high flexibility of the main-chain is responsible for the erasing process during irradiation, a poly (chloromethyl styrene) substituted with 4-phenylazophenol was synthesized (Sample 4 – Table 1). The erasing process was also identified in the case of the rigid chain Azo-PCMS, as shown in Figure 5 (film thickness 550 nm). In this case the amplitudes reached 100 and 40 nm after sample illumination for 45 and 90 minutes, respectively.

These experimental results are in support of the concept that multiple processes co-exist during the SRG inscription of the azo-polymers.

Experimental

Synthetic procedures

The polysiloxane containing chlorobenzyl groups in the side-chain was obtained by a two-step reaction, starting from dichloro(4-chloromethylphenylethyl)methylsilane. A hydrolysis reaction takes place in the first step, with the formation of a mixture of linear and cyclic oligomers. The second step ensures a cationic equilibration in the presence of trifluoromethane-sulfonic acid and 1,3-divinyl-1,1,3,3-tetramethyldisiloxane as chain blocker resulting in formation of linear polymers (Mn around 6,000). The polysiloxanes are then modified with different azophenols using a SN2 reaction, in DMSO. Details concerning polysiloxanes synthesis and characterization were previously reported.[45]

The poly(chloromethyl styrene) was obtained by a classical radical polymerization in solution (benzene) at 80°C using 2-2'-azoisobutyronitrile as initiator (Mn = 5,100). The PCMS was modified with 4-phenylazophenol in similar conditions as in the case of the polysiloxanes.

Rheological measurements

The rheological measurements were performed on a Physica MCR 501 rheometer (Anton Paar, Austria) equipped with electronically commutated synchronous motor, allowing rheological measurements in controlled-stress and controlled-strain modes and a Peltier device for the temperature control. The temperature can be adjusted between -40 and 200 °C. For regular tests parallel plate geometry with serrated plates was used to avoid slippage of the sample. The upper plate made of stainless steel has 50 mm in diameter. Simultaneous UV irradiation and rheological studies could be performed using an advanced UV system, under a Peltier controlled P-PTD-UV chamber on Physica MCR 501 rheometer. As measuring system a 43 mm parallel glass plate fixture was used. The UV source was an Omnicure Series 1000 manufactured by EXFO (Vanier, QC, Canada), using a 100 W lamp able to deliver UV light of 365 nm using a Hg bulb.

Viscoelasticity mapping during UV irradiation in dark

All experiments have been done using a Cypher S AFM (Asylum Research/ Oxford Instruments, Santa Barbara, CA) in AM-FM (Amplitude Modulation-Frequency Modulation) viscoelastic mapping mode employing Multi75-G (Budget Sensors, Bulgaria) probes with nominal resonance frequency fN = 75 kHz and nominal spring constant kN = 3 N/m. All probes have been mounted in a high frequency/ low noise AMFM cantilever holder. For the AM pass probes were actuated to free air amplitude of 1.5 V, at the nominal resonant frequency and engaged at 800 mV set point. The second pass was done actuating for the second harmonic at approximately 1.2 MHz for free air amplitude of 100mV, while maintaining phase to 90 degrees. Sample engagement was done so that probe tapping was in repulsive mode at a phase less than 50 degrees for the AM pass. Irradiation was done employing a Maxima-ML-3500/FA (Spectroline, NY) lamp (λ = 365 nm) calibrated at 75 ± 10 mW/cm2 for a 15 cm working distance. Before sample analysis, the cantilever's conversion constant was determined fitting the Young's modulus (E = 1.526 GPa) of a known sample (UHMWPE-8456 standard reference material from National Institute of Standards and Technology, USA) at 22 ± 0.2°C. A typical experiment involves the simultaneous acquisition of topography data and the modulus mapping before, during and after irradiation of the sample with 365 nm light. The evolution of modulus with time graphs are generated by extracting the layer of 256x256 pixels and averaging by line for a scan rate of 1Hz.

Optical modulation of the polymer film surface

The azo-polymeric films were obtained by a spin coating technique. The films were illuminated with an interference pattern produced by the superposition of two coherent beams incident symmetrically onto the film with respect to the film surface normal direction (Figure S5). The beam delivered by a 488nm wavelength laser diode was incident onto a beam splitter and the resulting beams were superposed onto the film after reflection onto two mirrors. The resulting interference pattern showed a sinusoidal modulation of the intensity along the polymer surface. The intensity in both beams was adjusted with optical densities to be equal. An average intensity of 180 mW·cm^{-2} was used for the experiments and the beam polarization was set on the incidence plane, i.e. perpendicular to the interference pattern fringes. A 633 nm wavelength Helium-Neon laser was employed to record the evolution of the 1rst order diffraction efficiency during the film illumination.

Fluorescence microscopy

To evaluate the adhesion properties of cells grown on the azo-polysiloxanic films, the architecture of the cytoskeleton structural elements was analysed by fluorescence microscopy, using human hepatoma derived cell line HepaRG. The cells were seeded on different polymer films, in 4% p-formaldehyde for 20 minutes at room temperature (22 °C) and incubated with the actin stain Alexa Fluor488-Phalloidin. Alternatively, the polymer films devoid of cells were directly stained with Alexa Fluor 488-labeled goat antibody. Images were taken with a Zeiss Axio Microscope using the AxioVision Rel 4.8 software.

Topography measurements by AFM

Topographic measurements evidencing the laser induced modulations on the polymer films were performed with a PicoLE 5100 AFM supplied by Agilent Technologies. The AFM was driven in the acoustically driven mode (tapping) in order to minimize the interaction of the tip with the surface during the scan. Arrow NCR Silicon probes from Nanoworld with nominal resonance frequency fN = 285 kHz and nominal spring constant kN = 42 N/m have been used. 512x512 pixels images were generated with a scan rate frequency of 0.2 to 0.4 Hz.

Conclusions

In this study we have shown the existence of photo-fluidity and demonstrated that the material viscosity upon interaction with UV/VIS light is strongly influenced by the polymer chemical structure. The presence of the photo-fluidization process during the light irradiation of azo-polymers was a subject of major debate between different research groups. The neglect of this process was, in our opinion, one of the reasons why the mass transport mechanism has not been completely elucidated until now. Recently however, an important number of research studies began to acknowledge the existence of photofluidity.[4, 17, 49, 50] The azo-polymers softening degree is expected to depend on the chemical structure, ranging from plastic to fluid state. Softening/fluidization is the first stage in the transformation of the irradiated material, preceding probably the mass displacement.

Another interesting process evidenced in the study is the relief erasure during the laser irradiation. Most likely, this behaviour is not induced by the polysiloxane high chain flexibility, as it was evidenced in the case of the rigid Azo-PCMS too (Tg = 87 °C).

Based on these results, a new mechanism of SRG formation is proposed, involving at least three processes: (1) the polymer photo-fluidization in the illuminated regions (2) the mass displacement from illuminated to the dark regions and (3) the inverse mass displacement from dark to the illuminated regions (Figure 6). These processes take place simultaneously, one or the other being dominant, depending on the polymer chemical structure and experimentation conditions. It must be highlighted that the inverse migration from dark to illuminated regions occurs only if the laser source is kept on. The erasure process stops once the laser is switched off.

A parallel study of the mechanical properties of the films, based on classical rheology and AFM, was also conducted in this investigation. The results evidenced important differences in the magnitude of elastic moduli as a function of film thickness. The polymer has an elastic behaviour when layered on thick films of approximately 400 microns, while acting as rigid

bodies in very thin films (500-2000 nm). This difference can be a consequence of the interactions with the glass substrate, which becomes more prominent in the case of thin films.

Having established this exciting behaviour of the azo-polymer films, future studies will focus on a systematic characterization of their interaction with cells and biomolecules. It is tempting to anticipate that these properties can be exploited to manipulate cellular growth and differentiation in a controlled manner, to unravel yet unknown molecular details of the complex cell-environment relationship.
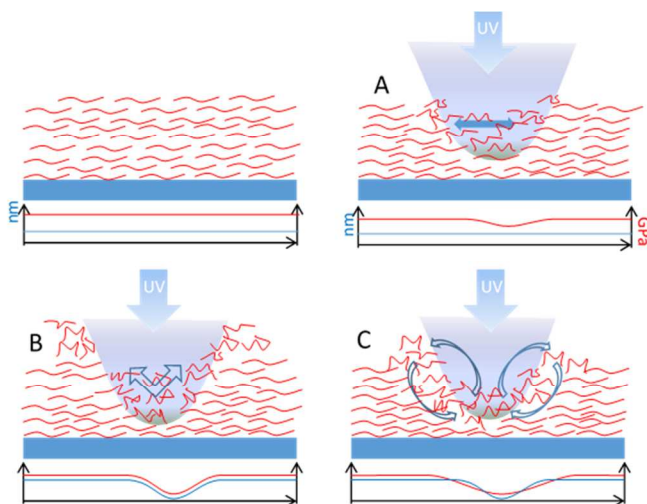

Fig.6 The proposed mechanism for SRG formation during laser irradiation, involving at least three processes: (A) the polymer photo-fluidization in the illuminated regions (B) the mass displacement from illuminate to the dark regions and (C) the inverse mass displacement from dark to the illuminated regions

Acknowledgements

Notes and references

[a] "Gheorghe Asachi" Technical University of Iasi, Department of Natural and Synthetic Polymers, Prof. Dimitrie Mangeron Street, 73, 700050-Iasi, Romania. E-mail: nhurduc@ch.tuiasi.ro

[b] Centre for Microbial Electrosynthesis at Advanced Water Management Centre, The University of Queensland, St Lucia, 4067, QLD, Australia. E-mail: b.donose@awmc.uq.edu.au

[c] Institute of Biochemistry of the Romanian Academy, Department of Viral Glycoproteins, Splaiul Independentei 296, Sector 6, 060041-Bucuresti, Romania. E-mail: nichita@biochim.ro

[d] CEA, LIST Saclay, Laboratoire Capteurs et Architectures Électroniques, F-91191 Gif-sur-Yvette, Cedex, France. E-mail: Licinio.ROCHA@cea.fr

1. P. Rochon, E. Batalla and A. Natansohn, *Appl Phys Lett*, 1995, **66**, 136-138.
2. D. Y. Kim, S. K. Tripathy, L. Li and J. Kumar, *Appl Phys Lett*, 1995, **66**, 1166-1168.
3. S. Ahmadi Kandjani, R. Barille, S. Dabos-Seignon, J.-M. Nunzi, E. Ortyland and S. Kucharski, *Nonlinear Optics, Quantum Optics: Concepts in Modern Optics*, 2007, **36**, 169-193.
4. A. Ambrosio, L. Marrucci, F. Borbone, A. Roviello and P. Maddalena, *Nat Commun*, 2012, **3**.
5. G. Di Florio, E. Brundermann, N. S. Yadavalli, S. Santer and M. Havenith, *Soft Matter*, 2014, **10**, 1544-1554.
6. A. Jacquart, E. Morin, F. Yang, B. Geffroy and E. Ishow, *Dyes Pigments*, 2012, **92**, 790-797.
7. S. Lee, H. S. Kang and J. K. Park, *Adv Mater*, 2012, **24**, 2069-2103.
8. F. L. Labarthet, T. Buffeteau and C. Sourisseau, *J Phys Chem B*, 1998, **102**, 2654-2662.
9. T. Ubukata, T. Seki and K. Ichimura, *Adv Mater*, 2000, **12**, 1675-+.
10. M. Saiddine, V. Teboul and J. M. Nunzi, *J Chem Phys*, 2010, **133**.
11. N. Mechau, M. Saphiannikova and D. Neher, *Appl Phys Lett*, 2006, **89**.
12. J. M. Ilnytskyi, M. Saphiannikova, D. Neher and M. P. Allen, *Soft Matter*, 2012, **8**, 11123-11134.
13. P. Karageorgiev, D. Neher, B. Schulz, B. Stiller, U. Pietsch, M. Giersig and L. Brehmer, *Nat Mater*, 2005, **4**, 699-703.
14. C. J. Barrett, P. L. Rochon and A. L. Natansohn, *J Chem Phys*, 1998, **109**, 1505-1516.
15. J. Kumar, L. Li, X. L. Jiang, D. Y. Kim, T. S. Lee and S. Tripathy, *Appl Phys Lett*, 1998, **72**, 2096-2098.
16. O. Baldus and S. J. Zilker, *Appl Phys B-Lasers O*, 2001, **72**, 425-427.
17. A. Ambrosio, P. Maddalena and L. Marrucci, *Phys Rev Lett*, 2013, **110**.
18. C. Fiorini, N. Prudhomme, G. de Veyrac, I. Maurin, P. Raimond and J. M. Nunzi, *Synthetic Met*, 2000, **115**, 121-125.
19. T. G. Pedersen, P. M. Johansen, N. C. R. Holme, P. S. Ramanujam and S. Hvilsted, *Phys Rev Lett*, 1998, **80**, 89-92.
20. V. P. Toshchevikov, M. Saphiannikova and G. Heinrich, *J Chem Phys*, 2012, **137**.
21. V. Teboul, M. Saiddine, J. M. Nunzi and J. B. Accary, *J Chem Phys*, 2011, **134**.
22. M. L. Juan, J. Plain, R. Bachelot, P. Royer, S. K. Gray and G. P. Wiederrecht, *Acs Nano*, 2009, **3**, 1573-1579.
23. S. Lee, J. Shin, Y. H. Lee, S. Fan and J. K. Park, *Nano Lett*, 2010, **10**, 296-304.
24. D. Garrot, Y. Lassailly, K. Lahlil, J. P. Boilot and J. Peretti, *Appl Phys Lett*, 2009, **94**.
25. H. W. Baac, J. H. Lee, J. M. Seo, T. H. Park, H. Chung, S. D. Lee and S. J. Kim, *Mat Sci Eng C-Bio S*, 2004, **24**, 209-212.
26. R. Barille, R. Janik, S. Kucharski, J. Eyer and F. Letournel, *Colloid Surface B*, 2011, **88**, 63-71.

27. N. Hurduc, A. Macovei, C. Paius, A. Raicu, I. Moleavin, N. Branza-Nichita, M. Hamel and L. Rocha, *Mat Sci Eng C-Mater*, 2013, **33**, 2440-2445.

28. A. L. Berrier and K. M. Yamada, *J Cell Physiol*, 2007, **213**, 565-573.

29. D. H. Kim, P. P. Provenzano, C. L. Smith and A. Levchenko, *J Cell Biol*, 2012, **197**, 351-360.

30. Y. Mei, K. Saha, S. R. Bogatyrev, J. Yang, A. L. Hook, Z. I. Kalcioglu, S. W. Cho, M. Mitalipova, N. Pyzocha, F. Rojas, K. J. Van Vliet, M. C. Davies, M. R. Alexander, R. Langer, R. Jaenisch and D. G. Anderson, *Nat Mater*, 2010, **9**, 768-778.

31. S. N. Weng and J. P. Fu, *Biomaterials*, 2011, **32**, 9584-9593.

32. E. K. F. Yim, E. M. Darling, K. Kulangara, F. Guilak and K. W. Leong, *Biomaterials*, 2010, **31**, 1299-1306.

33. P. Friedl and D. Gilmour, *Nat Rev Mol Cell Bio*, 2009, **10**, 445-457.

34. P. M. Tsimbouri, R. J. McMurray, K. V. Burgess, E. V. Alakpa, P. M. Reynolds, K. Murawski, E. Kingham, R. O. C. Oreffo, N. Gadegaard and M. J. Dalby, *Acs Nano*, 2012, **6**, 10239-10249.

35. A. S. Brydone, M. J. Dalby, C. C. Berry, R. M. D. Meek and L. E. McNamara, *Biomed Mater*, 2011, **6**.

36. H. N. Kim, D. H. Kang, M. S. Kim, A. Jiao, D. H. Kim and K. Y. Suh, *Ann Biomed Eng*, 2012, **40**, 1339-1355.

37. K. Kulangara, Y. Yang, J. Yang and K. W. Leong, *Biomaterials*, 2012, **33**, 4998-5003.

38. J. Wiejak, P. M. Tsimbouri, P. Herzyk, M. J. Dalby, G. Hamilton and S. J. Yarwood, *Biomaterials*, 2013, **34**, 1967-1979.

39. P. Huh and S. C. Kim, *Electron Mater Lett*, 2012, **8**, 355-355.

40. M. Kim, B. Kang, S. Z. Yang, C. Drew, L. A. Samuelson and J. Kumar, *Adv Mater*, 2006, **18**, 1622-+.

41. H. S. Kang, S. Lee, S. A. Lee and J. K. Park, *Adv Mater*, 2013, **25**, 5490-5497.

42. T. Konig, V. V. Tsukruk and S. Santer, *Acs Appl Mater Inter*, 2013, **5**, 6009-6016.

43. J. Plain, G. P. Wiederrecht, S. K. Gray, P. Royer and R. Bachelot, *J Phys Chem Lett*, 2013, **4**, 2124-2132.

44. J. A. Schuller, E. S. Barnard, W. S. Cai, Y. C. Jun, J. S. White and M. L. Brongersma, *Nat Mater*, 2010, **9**.

45. K. Kazmierski, N. Hurduc, G. Sauvet and J. Chojnowski, *J Polym Sci Pol Chem*, 2004, **42**, 1682-1692.

46. N. Hurduc, R. Enea, D. Scutaru, L. Sacarescu, B. C. Donose and A. V. Nguyen, *J Polym Sci Pol Chem*, 2007, **45**, 4240-4248.

47. R. Garcia and R. Proksch, *Eur Polym J*, 2013, **49**, 1897-1906.

48. J. B. Accary and V. Teboul, *J Chem Phys*, 2013, **139**.

49. A. Ambrosio, A. Camposeo, P. Maddalena, S. Patane and M. Allegrini, *J Microsc-Oxford*, 2008, **229**, 307-312.

50. G. J. Fang, J. E. Maclennan, Y. Yi, M. A. Glaser, M. Farrow, E. Korblova, D. M. Walba, T. E. Furtak and N. A. Clark, *Nat Commun*, 2013, **4**.